nature immunology

An innate antiviral pathway acting before interferons at epithelial surfaces

Marie B Iversen[1,2], Line S Reinert[1,2,12], Martin K Thomsen[1,2,12], Ieva Bagdonaite[3], Ramya Nandakumar[1,2], Natalia Cheshenko[4], Thaneas Prabakaran[1,2], Sergey Y Vakhrushev[3], Malgosha Krzyzowska[5], Sine K Kratholm[1,2], Fernando Ruiz-Perez[6], Steen V Petersen[1], Stanislas Goriely[7], Bo Martin Bibby[8], Kristina Eriksson[9], Jürgen Ruland[10], Allan R Thomsen[11], Betsy C Herold[4], Hans H Wandall[3], Sebastian Frische[1], Christian K Holm[1,2,13] & Søren R Paludan[1,2,13]

Mucosal surfaces are exposed to environmental substances and represent a major portal of entry for microorganisms. The innate immune system is responsible for early defense against infections and it is believed that the interferons (IFNs) constitute the first line of defense against viruses. Here we identify an innate antiviral pathway that works at epithelial surfaces before the IFNs. The pathway is activated independently of known innate sensors of viral infections through a mechanism dependent on viral O-linked glycans, which induce CXCR3 chemokines and stimulate antiviral activity in a manner dependent on neutrophils. This study therefore identifies a previously unknown layer of antiviral defense that exerts its action on epithelial surfaces before the classical IFN response is operative.

Many infectious agents enter the body through routes lined with epithelium, and the mucosal surfaces therefore represent the first barrier to infection. This is true for human viral pathogens such as herpes simplex virus (HSV), HIV and influenza A virus[1,2].

The immune defense against infections comprises a rapid innate immune response followed by a slowly evolving adaptive immune response, which serves an important role in protection of the host from subsequent reinfections with the same pathogen[3]. The innate immune system senses infections through pattern-recognition receptors (PRRs), which detect molecules that are unique to microbes or that are used by both the host and the microbe but present in abnormal locations[4]. Collectively, the microbial molecules stimulating innate immune activation are termed microbe-associated molecular patterns (MAMPs)[5]. Many classes of PRRs have been described, including membrane-bound Toll-like receptors (TLRs), intracellular RIG-I–like receptors (RLRs) and DNA sensors. PRR engagement stimulates antimicrobial activity and contributes to elimination of infection but can also lead to excessive inflammation[6–9]. In the case of viral infection, interferons (IFNs) and natural killer (NK) cells are of particular importance for early control and prevention of spread. IFNs exert antiviral activity by inducing expression of IFN-stimulated genes (ISGs), which restrict virus replication directly or indirectly via activation of cellular immune activities.

HSV is the cause of genital herpes, and type 2 (HSV-2) is responsible for the majority of cases worldwide[10]. HSV infects skin or mucosal surfaces and replicates lytically in epithelial cells then establishes latency in neuronal cells. To gain access to epithelial cells, HSV must traverse the mucosal layer. Innate immune sensing of HSV is known to involve TLR2, TLR3 and TLR9 as well as RLRs and DNA sensors[6,11–16]. The viral molecules detected by PRRs are thought to be glycoproteins, RNA and viral genomic DNA[17].

Although the role of IFNs in antiviral defense is well established[18–20], it is not known whether there are other innate antiviral mechanisms that work in parallel or even before the action of IFNs at the mucosa. Here we show that the chemokines CXCL9 and CXCL10 are induced during HSV infections before production of IFNs. This induction proceeds independently of the key innate immune response transcription factors IRF3 and IRF7, and it does not operate through a pathway involving known HSV-sensing PRRs. Viral stimulation of early CXCL10 expression relied on intact O-linked glycosylation of the virions. Mice lacking CXCR3, the receptor for CXCL9 and CXCL10, showed high viral load at early time points after HSV-2 infection. CXCL10 was produced by the epithelial cells and stimulated recruitment

[1]Department of Biomedicine, University of Aarhus, Aarhus, Denmark. [2]Aarhus Research Center for Innate Immunology, University of Aarhus, Aarhus, Denmark. [3]Department of Cellular and Molecular Medicine, Centre for Glycomics, University of Copenhagen, Copenhagen, Denmark. [4]Department of Pediatrics and Microbiology, Albert Einstein College of Medicine, New York, USA. [5]Department of Regenerative Medicine, Military Institute of Hygiene and Epidemiology, Warsaw, Poland. [6]Department of Pediatrics, University of Virginia School of Medicine, Charlottesville, Virginia, USA. [7]Institute for Medical Immunology, Université Libre de Bruxelles, Gosselies, Belgium. [8]Department of Biostatistics, University of Aarhus, Aarhus, Denmark. [9]Department of Rheumatology and Inflammation Research, University of Gothenburg, Gothenburg, Sweden. [10]Institut für Klinische Chemie und Pathobiochemie, Klinikum rechts der Isar, Technische Universität München, Munich, Germany. [11]Department of Immunology and Microbiology, University of Copenhagen, Copenhagen, Denmark. [12]These authors contributed equally to this work. [13]These authors jointly directed this work. Correspondence should be addressed to S.R.P. (srp@biomed.au.dk).

Received 7 July; accepted 9 October; published online 30 November 2015; doi:10.1038/ni.3319

of neutrophils in a CXCR3-dependent manner. Thus, we have identified an innate antiviral pathway at epithelial surfaces that acts before the function of IFNs.

RESULTS

Early expression of CXCR3 ligands after HSV infection

To characterize the early innate immune response to virus infection at epithelial surfaces, we infected wild-type C57BL/6 mice intravaginally with HSV-2 (strain 333, propagated in Vero African green monkey cells). We isolated vaginal washes on days 1–3 after infection (days 1–3 p.i.) to analyze viral mRNA and cytokines. Infectious virus was detectable in the washes at all three time points and peaked on day 2 (**Fig. 1a**). Staining of histological sections with antibodies to HSV (anti-HSV) revealed distinct regions, exclusively in the upper epithelial layer, that contained multiple infected cells, which is consistent with previous reports[21]. We also observed that viral gene products started to accumulate to detectable levels between 6 and 16 h after infection (**Fig. 1b**). Despite inoculation with viral MAMPs on the day of infection and the clear replication within the first 24 h, we did not detect type I interferon (IFN-α/β) activity in vaginal washes until day 2 p.i. (**Fig. 1c**). Type II interferon (IFN-γ) was produced, with kinetics resembling the expression of IFN-α/β (**Fig. 1d**), whereas type III interferon (IFN-λ) was not produced in detectable amounts in the infected vaginal tissue (**Fig. 1e**). Furthermore, reverse transcription–quantitiative PCR (RT-qPCR) analysis of *Ifnb* (encoding IFN-β) and *Ifna4* (encoding IFN-α4) mRNA in vaginal tissue isolated 0, 4 or 24 h after infection (h p.i.) showed no elevation of these transcripts (**Fig. 1f**). Hence, IFN production was not induced during completion of the first HSV-2 replication cycle (about 18 h) at the epithelial surface.

Despite the absence of IFN expression, we observed induction of the chemokines CXCL9 and CXCL10 at day 1 p.i. (**Fig. 1f–h**). These two chemokines act through the receptor CXCR3 and can be induced by IFN as well as through inflammatory signaling pathways[22]. CXCL10 production was not induced in samples from control mice administered PBS (**Supplementary Fig. 1a**). HSV-2 propagated in mouse neurons retained the capacity to evoke CXCL10 expression (**Supplementary Fig. 1b**), suggesting that the induction of CXCL10 was not an artifact of the virus's production in a species different from the organism challenged with the infection. The induction of CXCR3 ligands seemed to be specific, as the amounts of other chemokines and cytokines were not affected by HSV-2 infection at day 1 p.i. (**Fig. 1i** and **Supplementary Fig. 1c–k**). When we used a clinical isolate of HSV-2 in the mouse model, we observed the same effect, with induction of CXCL10 at day 1 p.i. and accumulation of IFN-α/β on day 2 but not day 1 (**Fig. 1j,k**). We also observed CXCL10 expression that preceded type I IFN expression in mice after ocular infection with HSV-1 (**Supplementary Fig. 2a**). Thus, after HSV infection, CXCR3 chemokines are produced early at epithelial surfaces, before the production of IFNs.

CXCR3 deficiency confers early elevated viral load

We next examined whether *Cxcr3*$^{-/-}$ mice were more susceptible to vaginal HSV-2 infection and whether this correlated with the observations in *Ifnar1*$^{-/-}$ mice, which are deficient in IFN-α/β receptor (IFNAR1). Vaginal washes from *Cxcr3*$^{-/-}$ mice showed elevated viral load at day 1 p.i. but not at day 2 p.i. (**Fig. 2a**); washes from the *Ifnar1*$^{-/-}$ mice and wild-type mice were indistinguishable at day 1 p.i., but those from *Ifnar1*$^{-/-}$ mice contained significantly more virus on day 2 (**Fig. 2b**). Although we observed only a 3- to 4-fold difference in levels of infectious virus in the vaginal washes from wild-type and *Cxcr3*$^{-/-}$ mice on day 1 p.i., the viral gene expression in the tissue was more than tenfold higher in *Cxcr3*$^{-/-}$ mice (**Fig. 2c**). We also observed dependence on CXCR3 for early control of infection after corneal HSV-1 infection (**Supplementary Fig. 2b**). *Ifnar1*$^{-/-}$ mice retained the ability to induce expression of CXCL9 and CXCL10 on day 1 p.i. (**Fig. 2d,e**),

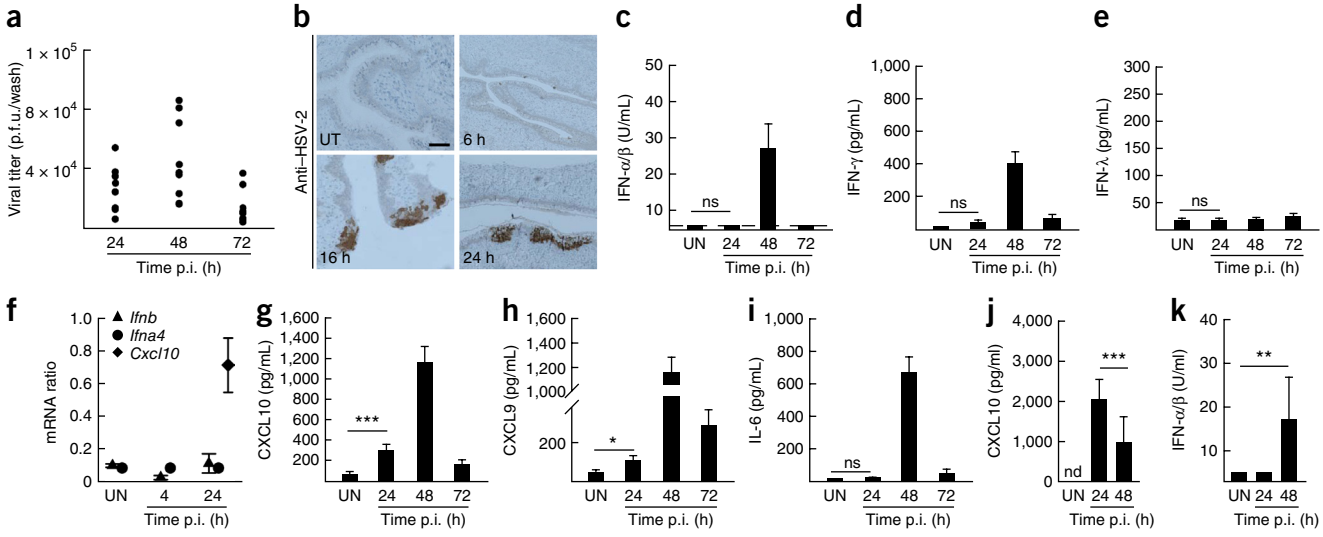

Figure 1 Vaginal HSV-2 infection induces early production of CXCR3 chemokines. (**a**) Plaque assay for viral load in vaginal washes from C57BL/6 mice infected intravaginally with 6.7×10^4 plaque-forming units (p.f.u.) of HSV-2 (strain 333) and isolated at different time points after infection. Data points represent individual mice ($n = 9$ per group). (**b**) Anti–HSV-2 staining of vaginal tissue sections from mice uninfected or infected for 6, 16 or 24 h. Scale bar, 100 μm. (**c**–**e**,**g**–**i**) Expression of IFN-α/β (IFN-α/β), IFN-γ, IFN-λ, CXCL10, CXCL9 and IL-6 in vaginal washes from mice infected as in **a**. $n = 6$–10 mice per group. (**f**) RT-qPCR analysis of CXCL10, IFN-β and IFN-α4 expression in vaginal tissue of uninfected mice and mice infected for 4 or 24 h. Data are normalized ratios, relative to GAPDH. $n = 3$ mice per group. (**j**,**k**) CXCL10 (**j**) and bioactive IFN-α/β (**k**) in vaginal washes from C57BL/6 mice infected intravaginally with 6.7×10^4 p.f.u. HSV-2 (clinical isolate 90.036). $n = 8$ mice per group. $^*P < 0.05$, $^{**}P < 0.01$, $^{***}P < 0.001$ (Wilcoxon rank-sum test). ns, not significant. Data are representative of 6 (**a**), 3–5 ((**c**–**e**, **g**–**i**) or 3 (**b**,**f**,**j**,**k**) experiments; error bars, mean ± s.d. (**c**–**k**)); UN, uninfected; nd, not detectable.

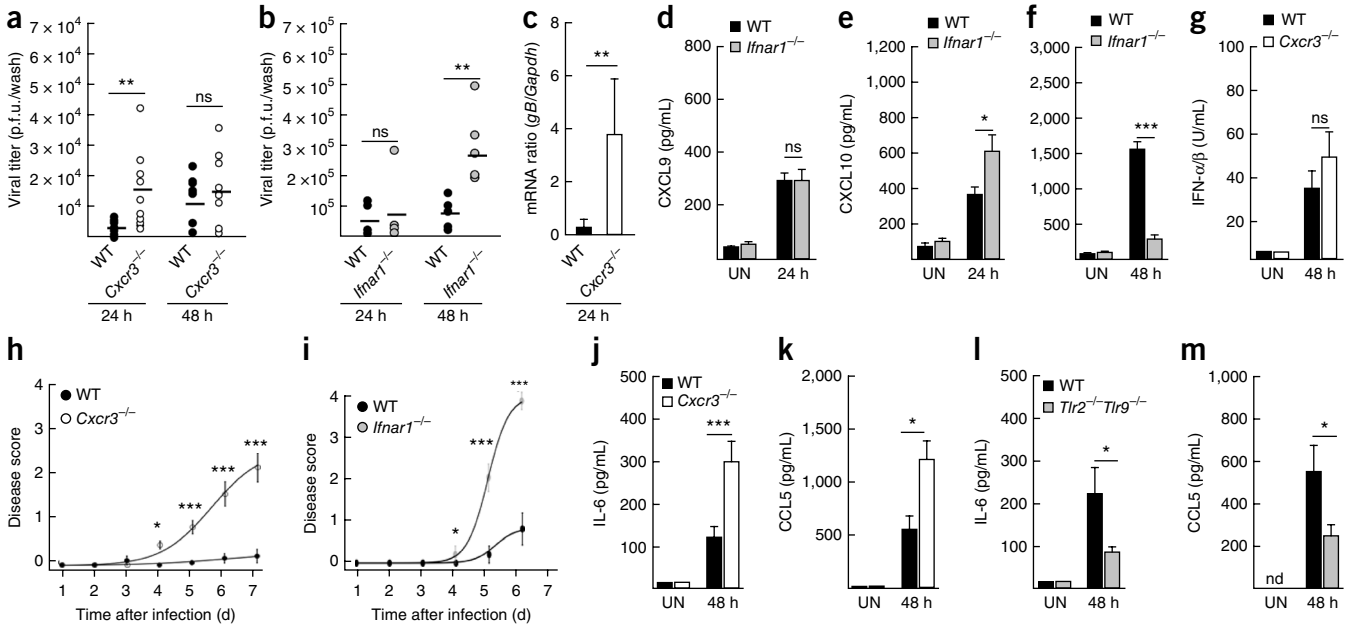

Figure 2 CXCR3 is essential for early antiviral defense before the requirement for the IFN-α/β system. (**a**–**g**) Wild-type (WT) C57BL/6, *Cxcr3*$^{-/-}$ and *Ifnar1*$^{-/-}$ mice were infected intravaginally with 6.7×10^4 p.f.u. of HSV-2. (**a**,**b**,**d**–**g**) Vaginal washes were isolated 24 h and 48 h p.i. and analyzed for viral load (**a**,**b**), CXCL9 concentration (**d**), CXCL10 concentration (**e**,**f**) and type I inteferon bioactivity (**g**). $n = 10$ (**a**,**g**) or 5 (**b**,**d**–**f**) mice per group. (**c**) *gB* mRNA measured by RT-qPCR (presented as ratio normalized to *Gapdh*) in total RNA from vaginal tissue 24 h after infection. $n = 6$ mice per group. (**h**,**i**) Disease scores for WT and *Cxcr3*$^{-/-}$ and *Ifnar1*$^{-/-}$ mice after HSV-2 infection. Data are presented as mean disease score ± s.d. and the calculated mean fit curve used for statistical analysis ($n = 5$–10 mice per group). (**j**–**m**) IL-6 and CCL5 concentrations in vaginal washes isolated 48 h p.i. from C57BL/6, *Cxcr3*$^{-/-}$ and *Tlr2*$^{-/-}$*Tlr9*$^{-/-}$ mice. $n = 8$–10 mice per group. $^*P < 0.05$, $^{**}P < 0.01$, $^{***}P < 0.001$ (Wilcoxon rank-sum test (**a**,**c**,**d**–**f**,**j**–**m**), Wilcoxon rank-sum test and Student's two-tailed *t*-test (**b**), nonlinear mixed effects regression (**h**,**i**) or Student's two-tailed *t*-test (**g**). Data are representative of two (**c**,**j**–**m**), three (**a**,**b**,**d**–**f**,**h**,**i**) or four (**g**) experiments (horizontal lines indicate means (**a**,**b**); error bars, mean ± s.d. (**c**–**m**). ns, not significant; UN, uninfected; nd, not detectable.

whereas expression of CXCL10 on day 2 p.i. was largely dependent on IFNAR1 expression, although we observed a modest elevation of CXCL10 in *Ifnar1*$^{-/-}$ mice upon infection (**Fig. 2f**). Moreover, the production of IFN-α/β s on day 2 after HSV-2 infection was not affected in *Cxcr3*$^{-/-}$ mice (**Fig. 2g**). Both *Cxcr3*$^{-/-}$ and *Ifnar1*$^{-/-}$ mice developed more severe signs of disease than wild-type mice (**Fig. 2h**,**i**). Consistent with this, the elevated early viral load was associated with subsequent increased secretion of the inflammatory cytokines IL-6 and CCL5 in *Cxcr3*$^{-/-}$ mice, as compared to wild-type mice (**Fig. 2j**,**k**), and these cytokines were induced in a TLR2- and TLR9-dependent manner (**Fig. 2l**,**m**). Thus, early high MAMP levels lead to elevated subsequent TLR-dependent inflammatory gene expression. Mice deficient in receptors for IFN-λ and IFN-γ did not have defective viral clearance or altered disease development (**Supplementary Fig. 3**). These results indicate that a defective CXCR3 pathway leads to increased early susceptibility to HSV infection at

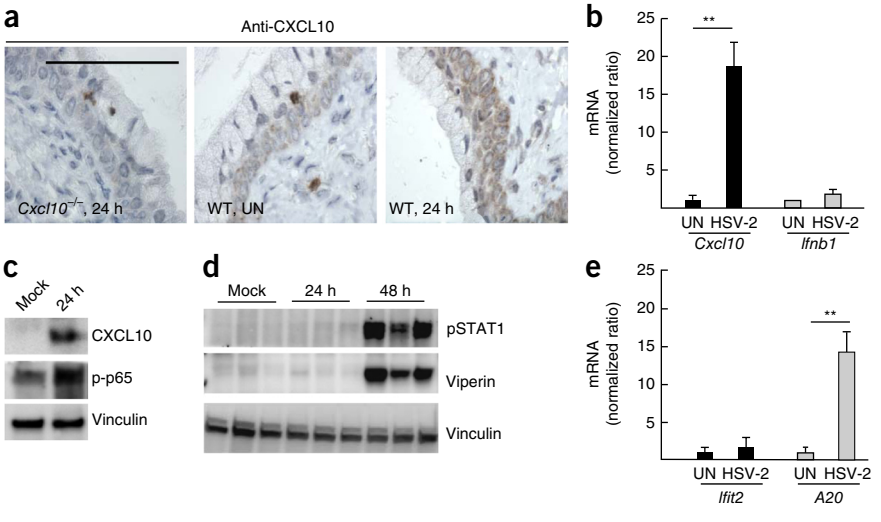

Figure 3 Early CXCL10 production is derived from vaginal epithelial cells. (**a**) Immunostaining for CXCL10 in vaginal tissue sections from WT and *Cxcl10*$^{-/-}$ mice uninfected (UN) or infected intravaginally with 6.7×10^4 plaque-forming units (p.f.u.) HSV-2 for 24 h (24 h p.i.). Scale bar, 100 μm. (**b**) Vaginal epithelial cell layers were isolated from C57BL/6 mice and cultured in the presence or absence of HSV-2 (6×10^6 p.f.u./ml) for 16 h. Total RNA was isolated and subjected to RT-qPCR using primers for *Cxcl10* and *Ifnb* mRNA. Data are presented as ratios normalized to *Gapdh* ($n = 4$ mice per group). (**c**,**d**) Immunoblot analysis of CXCL10, phosphorylated p65 (p-p65), phosphorylated STAT1 (pSTAT1), viperin and vinculin expression in vaginal epithelial lysates isolated from C57/BL6 mice infected intravaginally with 6.7×10^4 p.f.u. HSV-2 for 24 or 48 h. $n = 1$ (**c**); $n = 3$ (**d**). (**b**,**e**) RT-qPCR analysis of *Ifit2* and *A20* mRNAs expression in vaginal epithelial cell layers isolated from C57BL/6 mice and cultured in the presence or absence of HSV-2 (6×10^6 p.f.u./ml) for 16 h. $^{**}P < 0.01$ (Wilcoxon rank-sum test (**b**,**e**)). Data are representative of three (**b**–**d**) or two (**a**,**e**) experiments (ratios normalized to *Gapdh* ± s.d.; $n = 4$ mice per group (**b**,**e**)); UN, uninfected.

epithelial surfaces before any overt effects of IFNAR1 deficiency on viral control.

Early CXCL10 production is mediated by epithelial cells

Next we investigated which cells produced CXCL10 early after infection. Immunohistochemical staining of vaginal sections with anti-CXCL10 showed that epithelial cells were a prime source of CXCL10 and that CXCL10 expression was elevated in tissue from HSV-2–infected mice (**Fig. 3a**). We also observed that the cells producing CXCL10 were not restricted to the group productively infected with HSV-2 (**Figs. 3a** and **1b**). To confirm that epithelial cells were a source of early CXCL10 expression, we isolated and cultured vaginal epithelial cell layers from mice. The cells cultured *in vitro* expressed mucins and harboured a mucosal layer (**Supplementary Fig. 4**). After a period of rest in culture, the cells were infected with HSV-2. Similarly to our findings *in vivo*, expression of *Cxcl10* by the epithelial cell layer was detectable at 24 h p.i., before the induction of *Ifnb* (**Fig. 3b,c**). The delayed nature of the classical IFN response relative to CXCL10 expression in the tissue was confirmed by the detection of phosphorylated (phospho)-STAT1 (a marker of IFN activity) and viperin (encoded by an ISG) at 48 h p.i. but not at 24 h p.i. (**Fig. 3d**). The early expression of CXCL10 correlated with activation of the transcription factor NF-κB pathway by phosphorylation of subunit RelA (p-p65) in the epithelial tissue (**Fig. 3c**). Further characterization of gene expression at 24 h p.i. showed that expression of the NF-κB–stimulated gene *A20* (also known as *Tnfaip3*) but not the

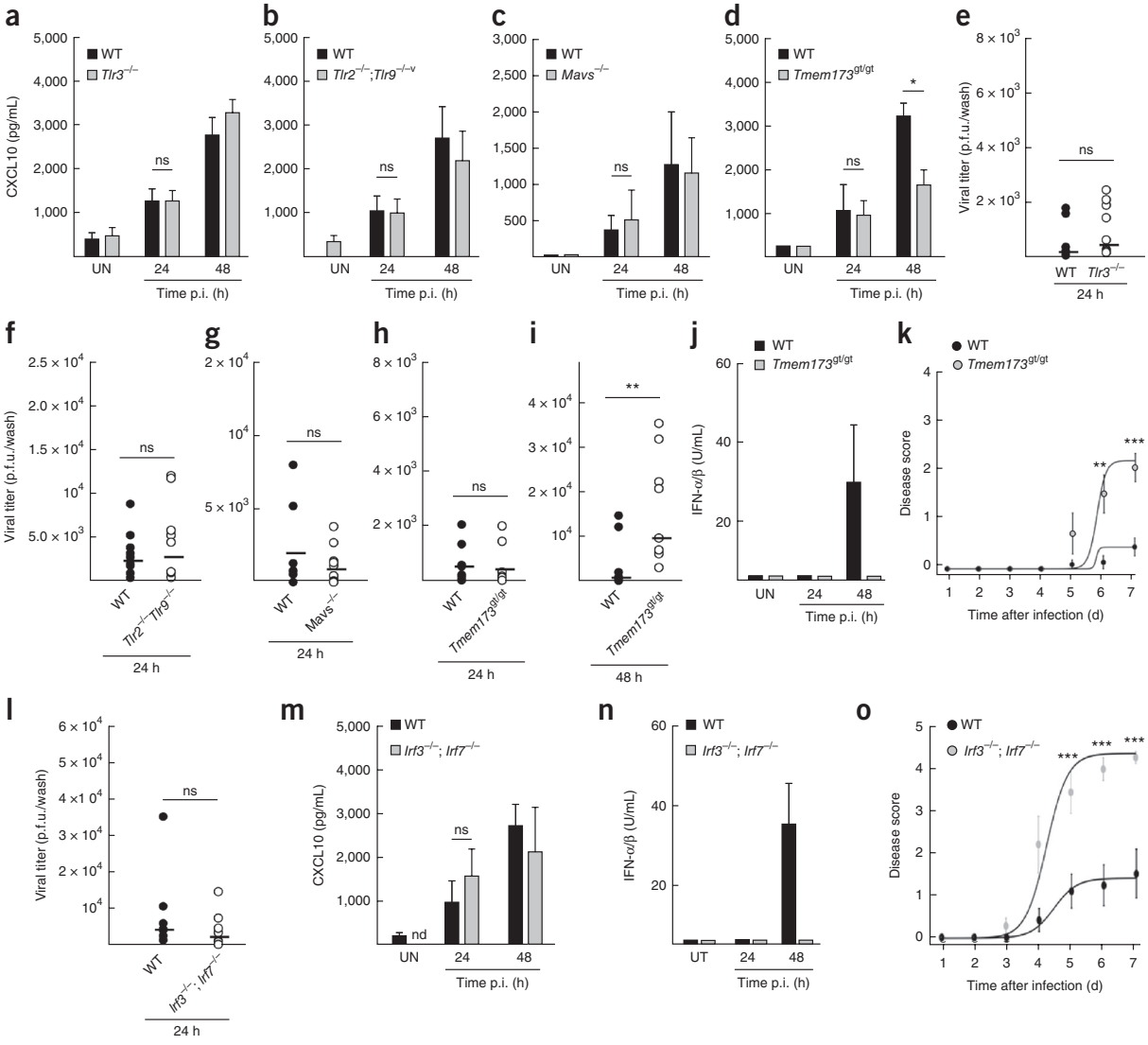

Figure 4 Early CXCL10 production is independent of known innate sensors recognizing HSV. (**a**–**d**) CXCL10 concentration in vaginal washes isolated from C57BL/6 wild-type (WT), *Tlr3*$^{-/-}$, *Tlr2*$^{-/-}$; *Tlr9*$^{-/-}$, *Mavs*$^{-/-}$ and *Tmem173*$^{gt/gt}$ mice infected intravaginally with 6.7×10^4 p.f.u. of HSV-2 at different time points. (**e**–**i**) Viral load in vaginal washes 24 h p.i. (**e**–**h**) or 48 h p.i. (**i**). Data points represent individual mice treated as in **a** ($n = 8$–10 mice per group). (**j**) IFN-α/β activity in vaginal washes from WT and *Tmem173*$^{gt/gt}$ mice. (**k**) Disease score for C57/BL6 and *Tmem173*$^{gt/gt}$ mice after HSV-2 infection. (**l**–**o**) Viral load (**l**), CXCL10 concentration (**m**) and IFN-α/β concentration (**n**) in vaginal washes isolated from uninfected mice or 24 or 48 h p.i. from WT and *Irf3*$^{-/-}$; *Irf7*$^{-/-}$ mice infected intravaginally with 6.7×10^4 p.f.u. HSV-2 ($n = 8$ per group). (**o**) Disease score for C57BL/6 and *Irf3*$^{-/-}$; *Irf7*$^{-/-}$ mice after HSV-2 infection. $^*P < 0.05$, $^{**}P < 0.01$, $^{***}P < 0.001$ (Wilcoxon rank-sum test (**e**–**i**,**l**,**m**), Student's two-tailed *t*-test (**a**–**d**) or nonlinear mixed effects regression (**k**,**o**)). Data are representative of 4 (**a**–**d**) or 3 (**e**–**i**,**l**,**m**) experiments (horizontal lines indicate means (**e**–**i**,**l**); error bars, mean ± s.d. (**a**–**d**,**j**,**k**,**m**–**o**); calculated mean fit curve was used for statistical analysis in **o**). ns, not significant; UN, uninfected; nd, not detectable.

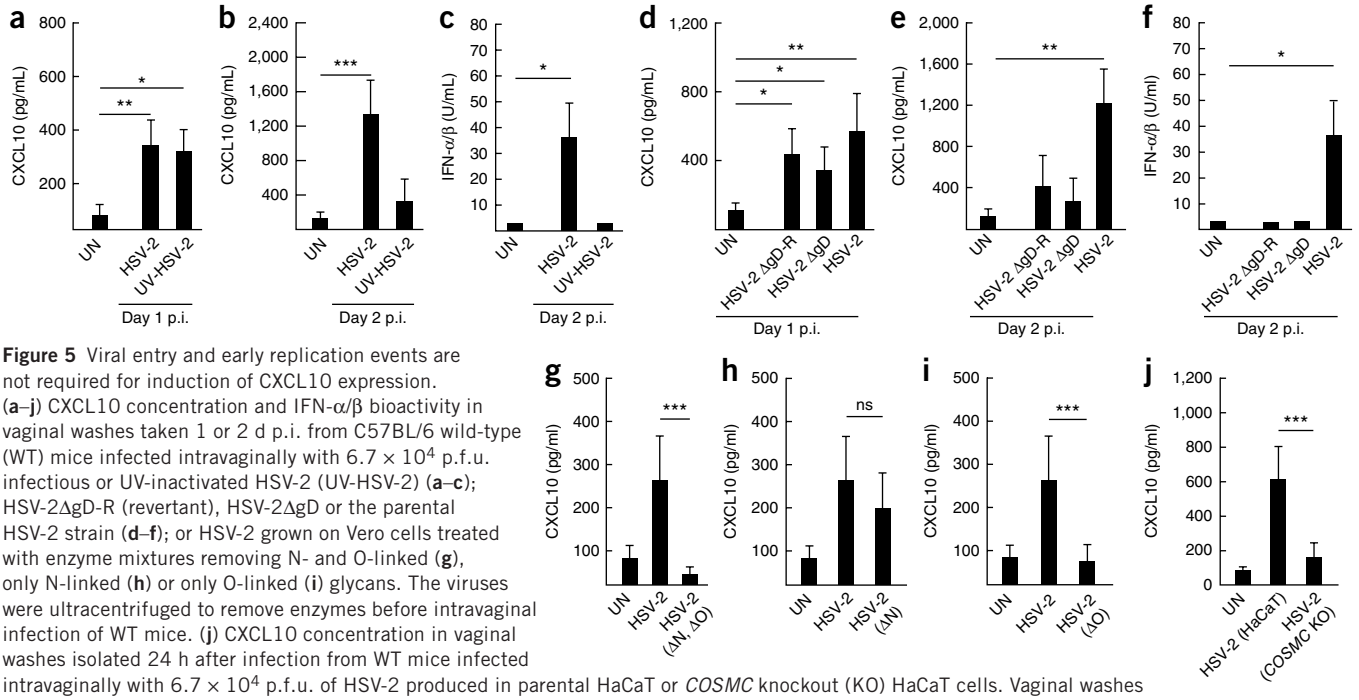

Figure 5 Viral entry and early replication events are not required for induction of CXCL10 expression. (**a**–**j**) CXCL10 concentration and IFN-α/β bioactivity in vaginal washes taken 1 or 2 d p.i. from C57BL/6 wild-type (WT) mice infected intravaginally with 6.7×10^4 p.f.u. infectious or UV-inactivated HSV-2 (UV-HSV-2) (**a**–**c**); HSV-2ΔgD-R (revertant), HSV-2ΔgD or the parental HSV-2 strain (**d**–**f**); or HSV-2 grown on Vero cells treated with enzyme mixtures removing N- and O-linked (**g**), only N-linked (**h**) or only O-linked (**i**) glycans. The viruses were ultracentrifuged to remove enzymes before intravaginal infection of WT mice. (**j**) CXCL10 concentration in vaginal washes isolated 24 h after infection from WT mice infected intravaginally with 6.7×10^4 p.f.u. of HSV-2 produced in parental HaCaT or *COSMC* knockout (KO) HaCaT cells. Vaginal washes were isolated 24 h p.i. for **g**–**j**; $n = 8$ mice.*$P < 0.05$, **$P < 0.01$, ***$P < 0.001$ (two-tailed Student's *t*-test (**a**,**c**,**d**,**f**,**g**–**i**) or Wilcoxon rank-sum test (**b**,**e**,**j**). Data are representative of three experiments (error bars, mean ± s.d.) (**a**–**j**). ns, not significant; UN, uninfected.

IRF3-stimulated gene *Ifit2* was upregulated at 24 h p.i. (**Fig. 3e**). These data suggest that epithelial cells are the source of early CXCL10 expression, which correlates with activation of NF-κB and precedes the classical IFN response.

Early CXCL10 induction is independent of known sensors

An mRNA screen for expression of PRRs in vaginal tissue revealed expression of all known HSV-sensing PRRs (**Supplementary Fig. 5a**). To address which sensing pathways are involved in early sensing of genital HSV-2 infection, we measured CXCL10 levels in vaginal washes from wild-type mice and mice deficient in TLR3 (*Tlr3*$^{-/-}$), TLR2 and TLR9 (*Tlr2*$^{-/-}$; *Tlr9*$^{-/-}$), the signaling adaptor MAVS (*Mavs*$^{-/-}$) or the membrane-associated adaptor STING (*Tmem173*$^{gt/gt}$). Lack of these HSV-sensing systems did not affect HSV-2–induced CXCL10 expression on day 1 p.i. (**Fig. 4a**–**d**). Correspondingly, none of these mice showed elevated viral load on day 1 p.i. (**Fig. 4e**–**h**). However, *Tmem173*$^{gt/gt}$ mice, like *Ifnar1*$^{-/-}$ mice, showed elevated viral load on day 2 p.i. (**Fig. 4i**) as well as low production of IFN-α/β and accelerated development of disease (**Fig. 4j**,**k**). *Irf3*$^{-/-}$; *Irf7*$^{-/-}$ mice did not have elevated viral load on day 1 p.i. and retained the ability to induce CXCL10 after infection, which further indicates that early CXCL10 expression is induced independently of the IFN pathway (**Fig. 4l**,**m**). By contrast, *Irf3*$^{-/-}$; *Irf7*$^{-/-}$ mice did not produce IFN on day 2 p.i. and developed severe signs of disease (**Fig. 4n**,**o**). Thus, the early production of CXCL10 in the genital tract of HSV-infected mice was derived from epithelial cells and induced through a pathway independent of known innate HSV-sensing systems.

CXCL10 expression relies on O-linked glycans on the virions

To address how epithelial cells sense HSV-2, we examined the requirement for viral replication. Mice were administered infectious or UV-inactivated virus, and CXCL10 was measured in vaginal washes. Both infectious and UV-inactivated virus induced CXCL10 expression on day 1 p.i. (**Fig. 5a**), but only the replication-competent virus stimulated expression of CXCL10 and IFN-α/β on day 2 p.i. (**Fig. 5b**,**c**). To examine the requirement for viral entry, we infected mice with

Table 1 O-glycosylation sites identified on individual HSV-2 envelope glycoproteins

Protein name	Uniprot ID[a]	Total sites	Unambiguous sites	T (Hex-HexNAc)	Tn (HexNAc)	List of O-glycosylated amino acid positions[b]
gB	P08666	13	11	9	10	39, 48, 55, 58, 59, 76, 84, 91, 260–274(1x), 475, 484, 494–495(1x), 700
gC	Q89730	14	11	12	13	42, 47–49(1x), 58, 59, 61, 71, 74, 75, 84, 89, 90, 91, 130–145(1x), 398–399(1x)
gD	Q69467	1	1	1	0	255
gE	P89475	3	3	3	2	203, 212, 396
gG	P13290	18	14	13	14	147–158(2x), 205, 325, 353-356(1x), 362, 450, 454–455(1x), 461, 464, 527, 530, 533, 537, 549, 586, 603, 616
gH	P89445	1	1	0	1	162
gI	P13291	6	5	6	6	208, 212, 213, 214, 223, 229–231(1x)
gJ	P13293	1	1	1	0	40
gK	P22485	1	0	1	0	64–78(1x)
gL	P28278	5	3	4	3	120–121(1x), 141, 154–155(1x), 194, 202

[a]UniProt IDs of reference HSV-2 strain (HG52) are provided owing to incomplete annotation of the strain 333 proteome. [b]Numbering according to reference HSV-2 strain. Hex, hexose; HexNAc, *N*-acetylhexosamine; 1×, one ambiguous glycosite within indicated peptide stretch.

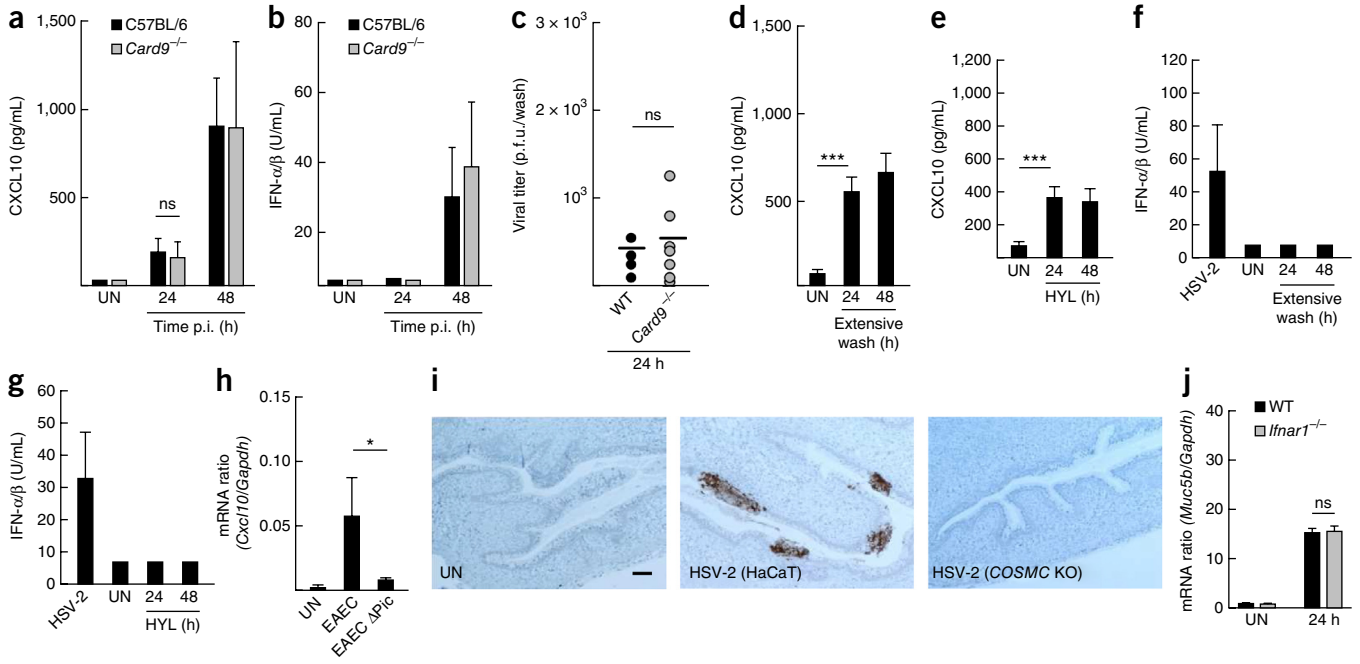

Figure 6 Disturbance of mucosal integrity induces IFN-independent CXCL10 expression. (**a**–**c**) CXCL10 concentration (**a**), type I interferon bioactivity (**b**) and virus titers (**c**) in vaginal washes from C57BL/6 wild-type (WT) and *Card9*$^{-/-}$ mice infected intravaginally with 6.7×10^4 p.f.u. of HSV-2. Washes were isolated 24 or 48 h p.i. (**d**–**g**) CXCL10 concentration (**d**,**e**) and IFN-α/β bioactivity (**f**,**g**) in vaginal washes isolated 24 or 48 h p.i. from mice flushed intravaginally three times with PBS (extensive wash) or treated with hyaluronidase (HYL; **e**,**g**). $n = 6$–8 mice per group. (**h**) *Cxcl10* mRNA determined by RT-qPCR in total RNA from vaginal tissue culture slices stimulated with 1×10^6 of EAEC or EAEC ΔPic per well in 96-well plates. $n = 3$ mice per group. (**i**) HSV-2 immunostaining in vaginal tissue sections from uninfected mice or mice infected for 24 h with HSV-2 grown in parental or *COSMC* knockout (KO) HaCaT cells. Scale bar, 100 μm. (**j**) *Muc5b* mRNA expression (normalized to *Gapdh*) in total RNA from vaginal tissue of WT and *Ifnar1*$^{-/-}$ mice infected for 24 h with HSV-2. $n = 6$ mice per group. $^*P < 0.05$, $^{***}P < 0.001$ (Wilcoxon rank-sum test). Data are representative of two experiments (**a**–**j**); error bars, mean and s.d. (**a**,**b**,**d**–**h**,**j**); horizontal lines indicate mean (**c**). ns, not significant; UN, uninfected.

HSV-2 lacking glycoprotein D (HSV-2ΔgD)[23], which is unable to enter cells, and found that this virus induced production of CXCL10 on day 1 p.i. but not CXCL10 or IFN-α/β on day 2 (**Fig. 5d**–**f**). Therefore, the early production of CXCL10 is independent of viral entry, whereas the stimulation of IFN-α/β and late CXCL10 requires *de novo* generation of virions in the tissue. Only mice infected with wild-type HSV-2 developed signs of disease, thus confirming that the viruses used were replication incompetent (**Supplementary Fig. 6**).

Because the early CXCL10 response was independent of viral entry, we wanted to examine the role of viral glycans, which are major surface-exposed components of the virus particle. First, we depleted HSV-2 of N-linked and O-linked glycans by treatment with PNGase F, which removes N-linked sugars, or a mixture of enzymes that target O-linked glycans (**Supplementary Fig. 7a**). The removal of O-linked sugars on HSV-2 led to impaired viral entry and production of fewer infectious progeny virus (**Supplementary Fig. 7b**,**c**). No differences between the viruses were observed with respect to stimulation of STING translocation, an indirect measure of activation of the DNA-sensing pathway (**Supplementary Fig. 7d**). Virus devoid of both N- and O-linked sugars did not evoke early CXCL10 expression (**Fig. 5g**). Whereas elimination of N-linked glycans from the virions did not affect virus-induced CXCL10 expression, virions stripped of O-linked sugars did not stimulate this response (**Fig. 5h**,**i**). To get complementary data on the role of O-linked glycans in HSV-2–induced CXCL10 expression, we made viral preparations in *COSMC* knockout cells, derived from the human keratinocyte cell line HaCaT engineered to lack the gene *C1GALT1C1* (also known as *COSMC*). These cells produce only truncated O-linked glycans[24]. Similarly to HSV-2 enzymatically depleted of O-linked sugars, HSV-2 grown in *COSMC* knockout cells showed impaired ability to stimulate early CXCL10 expression (**Fig. 5j**). These virions appeared to be as stable as the O-glycosylated virus, as measured by accumulation of capsid-free DNA in medium after incubation at 37 °C for 30 min in the absence of cells (**Supplementary Fig. 7e**). Early production of CXCL10 was not stimulated by heat-inactivated virus (data not shown), thus suggesting that O-linked glycans on intact virions stimulate the response. The impaired induction of CXCL10 on day 1 p.i. by viruses devoid of O-linked glycans was not observed on day 2 p.i. where CXCL10 was induced in a IFN-α/β –dependent manner (**Supplementary Fig. 7f**,**g** and **Fig. 2f**). Mass spectrometric mapping of the O-glycosylation sites on HSV-2 envelope proteins revealed 63 O-linked glycosylation sites on 10 HSV-2 envelope proteins (**Table 1** and **Supplementary Table 1**), and these results are similar to the published description of the HSV-1 O-glyproteome[25].

HSV-2 propagated in *COSMC* knockout cells showed modestly impaired ability to enter cells and replicated at lower virus titers than virus preparations made in wild-type HaCaT cells (**Supplementary Fig. 7b**,**h**), which confirms an essential role for O-linked sugars in viral replication, as was observed for viruses treated with enzymes to remove O-linked sugars. Collectively, these data suggest that HSV-2 induces early expression of CXCR3 chemokines through a mechanism dependent on O-linked sugars on the virions.

Disturbance of the mucus layer stimulates expression of CXCL10

The finding that HSV-2–induced expression of CXCR3 chemokines was dependent on O-linked sugars prompted us to examine the role of C-type lectin receptors (CLRs) in this early antiviral response. RT-qPCR showed that the majority of CLRs were expressed at very low

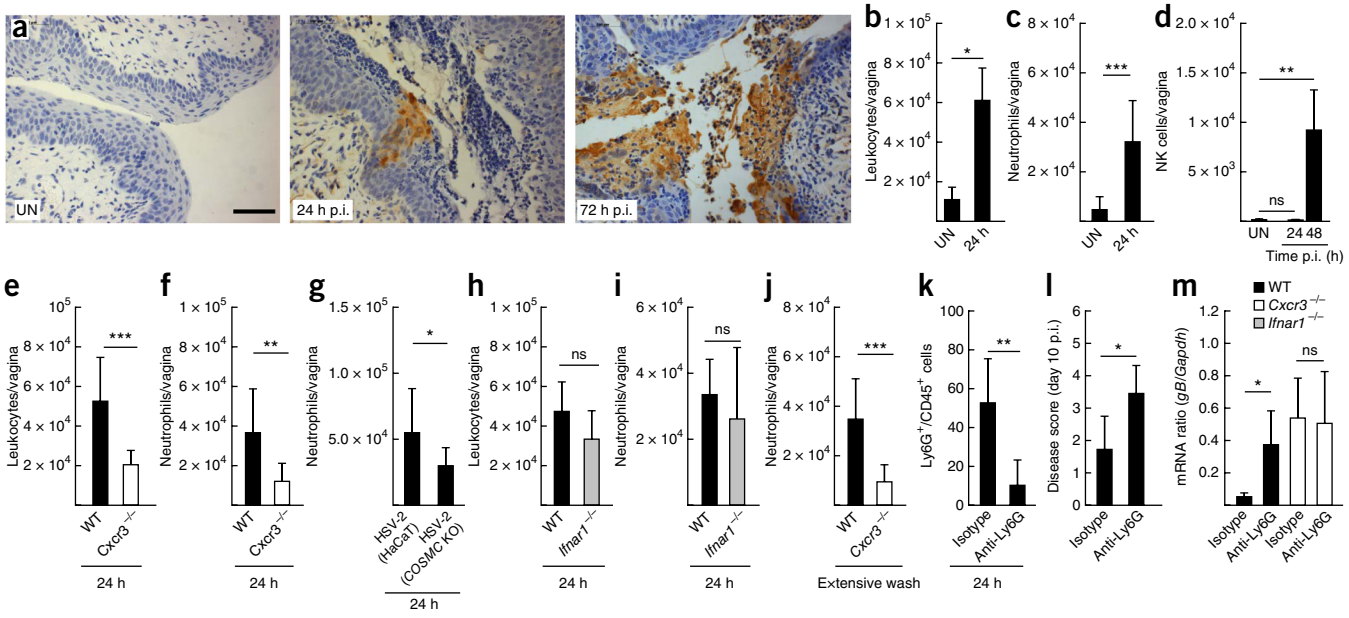

Figure 7 HSV-2 infection stimulates early recruitment of neutrophils in a CXCR3-dependent manner. (**a**) Hematoxylin staining and HSV-2 immunostaining in vaginal tissue sections from C57BL/6 wild-type (WT) mice infected intravaginally with 6.7×10^4 p.f.u HSV-2. Scale bar, 100 μm. (**b**–**j**) Average number of CD45$^+$ cells (leukocytes; **b**,**e**,**h**), Ly6G$^+$CD11b$^+$ cells (neutrophils; **c**,**f**,**g**,**i**,**j**) and CD45$^+$NK1.1$^+$ cells (NK cells; **d**) per vagina in WT, *Cxcr3*$^{-/-}$ and *Ifnar1*$^{-/-}$ mice infected with HSV-2 or flushed three times with PBS intravaginally. (**k**–**m**) Mice were treated with anti-Ly6G for 24 h before intravaginal infection with 6.7×10^4 p.f.u. of HSV-2. (**k**) Percentage of Ly6G$^+$CD11b$^+$ cells in single-cell leukocytes (CD45$^+$) isolated from vaginal tissue 24 h p.i. (**l**) Disease score on day 10 p.i. in infected mice treated with anti-Ly6G or isotype control. (**m**) HSV-2 *gB* mRNA levels (normalized to *Gapdh*) from total RNA isolated from vaginal tissue on day 1 p.i. Data are representative of three (**b**–**l**) or two (**a**,**m**) experiments with $n = 3$ (**b**,**d** uninfected), 10 (**c**,**d** infected groups), 6 (**g**), 9 (**e**,**f**,**h**,**i**), 4 (**j**), 5 (**k**) or 8 (**l**,**m**) mice per group (error bars, mean ± s.d. (**b**–**f**,**h**–**m**)).*$P < 0.05$, **$P < 0.01$, ***$P < 0.001$ (Student's two-tailed *t*-test (**b**,**d**) or Wilcoxon rank-sum test (**c**,**e**,**f**,**h**,**i**,**k**,**m**). ns, not significant; UN, uninfected.

levels in the vaginal tissue (**Supplementary Table 2**). Next we examined the role for the common CLR adaptor CARD9 in HSV-2–induced expression of CXCL10 and IFN-α/β in the vagina. *Card9*$^{-/-}$ mice demonstrated normal early IFN-independent CXCL10 production in virus-infected tissue, and the antiviral response was not affected by lack of CARD9 (**Fig. 6a**–**c**). These data suggest that CLRs are not responsible for the early IFN-independent innate response.

We next wanted to evaluate the response to sterile damage of the mucosa. We used two approaches: repeated flush of the genital tract with PBS or local treatment with hyaluronidase. Measurement of CXCL10 and IFN-α/β concentrations in vaginal washes isolated on days 1 and 2 p.i. showed that both treatments stimulated expression of CXCL10 but not IFN-α/β s on day 1 (**Fig. 6d**–**g**). As many bacteria disrupt mucosal integrity to allow establishment of infection, either via enzymes or physical action of flagella[26], we speculated that bacteria might also evoke CXCL10 expression through this pathway. To test this possibility *in vitro*, we cultured freshly isolated vaginal tissue with a wild-type strain of enteroaggregative *Escherichia coli* (EAEC) and an EAEC mutant lacking the mucinase Pic (EAEC ΔPic)[27]. Culture with wild-type EAEC stimulated expression of *Cxcl10* mRNA to a significantly greater degree than culture with the EAEC ΔPic strain (**Fig. 6h**). Finally, to examine the role of O-linked glycans in the ability of HSV-2 to penetrate the mucosal layer, we stained tissue sections from mice infected with HSV-2 produced in wild-type or *COSMC* knockout cells for HSV-2. Although the virus grown in parental HaCaT cells readily established replication foci in the epithelium, HSV-2 grown in *COSMC* knockout cells did not form detectable replication foci 24 h p.i. (**Fig. 6i**). However, we detected replication in mice on day 2 p.i., irrespective of which virus was used for the initial infection (data not shown). This suggests that O-linked sugars are essential both for the ability of the virion to efficiently cross the mucus layer and for optimal viral entry.

The early virus-induced IFN–independent genes expressed in vaginal tissue included *Muc5b*, encoding NF-κB–inducible mucin-5ab (**Fig. 6j**), which suggests that the early response to mucosal disturbance may also include repair activities. Collectively, these data demonstrate that CXCL10 expression at mucosal surfaces before the IFN-α/β response is stimulated by disruption of mucosal integrity.

Neutrophils exert early CXCR3-dependent antiviral activity

Last, we wanted to investigate the functional outcome of expression of CXCR3 chemokines early after genital HSV-2 infection. Tissue sections from uninfected and HSV-2–infected mice were stained with hematoxylin, and the presence of viral antigens in the tissue was visualized by immunostaining with anti-HSV. No leukocytes were found in the genital tract of uninfected animals (**Fig. 7a**). After 24 h of exposure to HSV-2, large amounts of infiltrating cells were present in the outer layer of the epithelium surrounding the infected foci (**Fig. 7a**). Next, we isolated total leukocytes from vaginal tissue and analyzed them by flow cytometry to quantify total leukocytes, neutrophils and NK cells (**Supplementary Fig. 8a**,**b**). This analysis confirmed the histological data on influx of leuocytes (**Fig. 7b**) and furthermore revealed significant elevation in the number of neutrophils in the vaginal tissue on day 1 p.i. (**Fig. 7c**). By contrast, the number of NK cells was not elevated 24 hp.i. but was high 48 h p.i. (**Fig. 7d**). Importantly, the increase in number of total leukocytes and neutrophils in vaginal tissue on day 1 p.i. was significantly smaller in *Cxcr3*$^{-/-}$ mice and in wild-type mice infected with virus devoid of O-linked glycans (i.e., grown in *COSMC* knockout cells) but was not affected in *Ifnar1*$^{-/-}$ mice (**Fig. 7e**–**i**). The difference in leukocyte

infiltation between wild-type and *Cxcr3*$^{-/-}$ mice was not seen in uninfected mice (data not shown). Similarly to viral infection, damaging of the epithelial cell layer by extensive washing also led to recruitment of neutrophils to the vagina in a CXCR3-dependent manner (**Fig. 7j**).

To examine the importance of neutrophils in prevention of viral disease, we depleted neutrophils *in vivo* using anti-Ly6G. This treatment efficiently prevented accumulation of neutrophils on day 1 p.i. but did not affect HSV-2–induced expression of CXCL10 (**Fig. 7k** and **Supplementary Fig. 8c**). Accordingly, mice treated with anti-Ly6G developed more severe signs of disease after genital HSV-2 infection (**Fig. 7l**), and we observed higher virus titer in wild-type (but not *Cxcr3*$^{-/-}$) mice treated with anti-Ly6G (**Fig. 7m**). Thus, early expression of CXCR3 chemokines before the expression of IFNs stimulates recruitment of leukocytes, including neutrophils, which exert protective responses.

DISCUSSION

In this study we have demonstrated the existence of an innate pathway that is activated by disturbance of the mucus layer and exerts antiviral activity before the action of the potent, but also potentially pathological, IFN system.

The finding that a CXCR3-dependent antiviral pathway operates before the induction of IFN-α/β through the STING pathway demonstrates the existence of antiviral mechanisms that act before the IFN-driven innate antiviral program. The IFN-independent CXCR3 chemokine-neutrophil pathway may have a role in preventing virus from establishing replication and thus affect the levels of MAMPs that accumulate. This could allow the host to eliminate infection without mounting a potentially immunopathologial IFN response. Our study thus identifies a mechanism wherein the presence of viruses at epithelial surfaces is detected before viral entry to stimulate a rapid and low-grade influx of neutrophils with antiviral activity into the tissue. Neutrophils are well known to possess potent antibacterial activity, and defects in optimal neutrophil activity are associated with susceptibility to certain bacterial infections and also bacteria-mediated immunopathology[28,29]. Although neutrophils are recruited to the vagina of HSV-2–infected mice and contribute to control of the virus[30], this cell type has not been thought to be involved in antiviral defense. However, with the identification of antiviral functions of neutrophils, this abundant, immunologically very active but short-lived cell type is emerging to have a more general role in host defense[31]. It will be interesting to learn whether the pathway described here has a function in the sensing of damage at mucosal surfaces to mount broad-spectrum defense activities and initiate repair activities.

With respect to the host sensing of HSV-2 in the vagina, we found that virus-induced CXCL10 expression on day 1 was induced independently of known HSV-sensing PRRs through a mechanism independent of viral entry. However, the early CXCL10 response was dependent on O-linked glycans, which were also essential for optimal replication of the virus *in vitro*. Therefore, O-linked sugars are essential for optimal HSV-2 replication, and loss of O-linked glycosylation would be associated with loss of fitness for the virus. In this respect, O-linked glycans on HSV partially fulfill the original description of MAMPs by Janeway[5]—they are essential for microbial growth and conserved among a wide range of microbes. However, the viral induction of early CXCL10 expression was independent of CLRs, as assessed in *Card9*$^{-/-}$ mice, which suggests that the response is not triggered by a direct sugar–PRR interaction. Rather, the early induction of CXCL10 expression could be mimicked by disturbance of the mucosa. These data suggest that the disturbance of the mucosal layer initiates low-grade NF-κB activation in the epithelium, thus stimulating expression of NF-κB–inducible genes, including *Cxcl9*, *Cxcl10*, *A20* and *Muc5b*[32,33]. Genes requiring activation of IRF3 and/or IRF7 or more robust NF-κB activation (for example, those encoding IFN-α/β and *Il6*) would be induced only later, when signaling from TLRs and intracellular PRRs is initiated. It is also notable that the set of early genes induced in an IFN-independent manner include the *Muc5b*, which suggests stimulation of activities to repair the damaged mucosal layer in addition to the antimicrobial activities. The mechanism of signaling in this response remains unresolved, but one possibility is mucin-dependent signaling in epithelial cells, which could be initiated by disruption of the inter-mucin interaction network[34]. Such a mechanism would work in a manner similar to the 'guard theory' in plant immunity, where innate immune responses are stimulated by the consequences of a virulence factor or pathogen rather than directly through recognition of a MAMP[35].

Here we identify an innate antiviral pathway that senses incoming viruses on epithelial surfaces by a mechanism dependent on viral O-linked glycans to stimulate expression of CXCR3 chemokines. This in turn leads to recruitment of neutrophils and execution of antiviral activity that precedes IFN activity. Because this early response is not associated with major inflammation or pathology, it probably allows the host to detect and eliminate microorganisms at mucosal surfaces without activating significant local or systemic reactions.

METHODS

Methods and any associated references are available in the online version of the paper.

Note: Any Supplementary Information and Source Data files are available in the online version of the paper.

ACKNOWLEDGMENTS

We thank K.S. Petersen and I.M. Poulsen for technical assistance and the AU FACS Core facility for technical help. Supported by The Danish Medical Research Council (12-124330 to S.R.P.; 1331-00133B to H.H.W.), the Novo Nordisk Foundation (S.R.P.), the Lundbeck Foundation (R34-3855 to S.R.P.), Aarhus University Research Foundation (S.R.P.), the EU FP7 Mobilex program (1333-00090A to M.K.T.), the US National Institutes of Health (AI065309 to B.C.H.), Faculty of Health Sciences, AU (M.B.I.), the Danish National Research Foundation (DNRF107 to H.H.W.), the Excellence Programme for Interdisciplinary Research (CDO2016 to H.H.W.), the German Research Foundation (DFG, SFB 1054 to J.R.) and the European Research Council (FP7, grant agreement 322865 to J.R.).

AUTHOR CONTRIBUTIONS

M.B.I., C.K.H. and S.R.P. conceived of the study; M.B.I., L.S.R., M.K.T., I.B., R.N., N.C., T.P., S.Y.V., M.K. and S.K.K. performed experiments; M.B.I., B.M.B., H.H.W., S.F., C.K.H. and S.R.P. analyzed data; F.R.-P., S.G., K.E., J.R., A.R.T., B.C.H., S.V.P. and H.H.W. provided reagents and intellectual guidance; and M.B.I. and S.R.P. wrote the paper.

COMPETING FINANCIAL INTERESTS

The authors declare no competing financial interests.

1. Iwasaki, A. Antiviral immune responses in the genital tract: clues for vaccines. *Nat. Rev. Immunol.* **10**, 699–711 (2010).
2. Ichinohe, T., Iwasaki, A. & Hasegawa, H. Innate sensors of influenza virus: clues to developing better intranasal vaccines. *Expert Rev. Vaccines* **7**, 1435–1445 (2008).
3. Medzhitov, R. Recognition of microorganisms and activation of the immune response. *Nature* **449**, 819–826 (2007).
4. Kawai, T. & Akira, S. Toll-like receptors and their crosstalk with other innate receptors in infection and immunity. *Immunity* **34**, 637–650 (2011).
5. Janeway, C.A. Jr. Approaching the asymptote? Evolution and revolution in immunology. *Cold Spring Harb. Symp. Quant. Biol.* **54**, 1–13 (1989).
6. Lund, J., Sato, A., Akira, S., Medzhitov, R. & Iwasaki, A. Toll-like receptor 9-mediated recognition of Herpes simplex virus-2 by plasmacytoid dendritic cells. *J. Exp. Med.* **198**, 513–520 (2003).

7. Kato, H. *et al.* Differential roles of MDA5 and RIG-I helicases in the recognition of RNA viruses. *Nature* **441**, 101–105 (2006).
8. Okabe, Y., Kawane, K., Akira, S., Taniguchi, T. & Nagata, S. Toll-like receptor-independent gene induction program activated by mammalian DNA escaped from apoptotic DNA degradation. *J. Exp. Med.* **202**, 1333–1339 (2005).
9. Imai, Y. *et al.* Identification of oxidative stress and Toll-like receptor 4 signaling as a key pathway of acute lung injury. *Cell* **133**, 235–249 (2008).
10. Gupta, R., Warren, T. & Wald, A. Genital herpes. *Lancet* **370**, 2127–2137 (2007).
11. Kurt-Jones, E.A. *et al.* Herpes simplex virus 1 interaction with Toll-like receptor 2 contributes to lethal encephalitis. *Proc. Natl. Acad. Sci. USA* **101**, 1315–1320 (2004).
12. Sørensen, L.N. *et al.* TLR2 and TLR9 synergistically control herpes simplex virus infection in the brain. *J. Immunol.* **181**, 8604–8612 (2008).
13. Reinert, L.S. *et al.* TLR3-deficiency renders astrocytes permissive to HSV infection and facilitates establishment of CNS infection in mice. *J. Clin. Invest.* **122**, 1368–1376 (2012).
14. Melchjorsen, J. *et al.* Innate recognition of HSV in human primary macrophages is mediated via the MDA5/MAVS pathway and MDA5/MAVS/Pol III independent pathways. *J. Virol.* **84**, 11350–11358 (2010).
15. Ishikawa, H., Ma, Z. & Barber, G.N. STING regulates intracellular DNA-mediated, type I interferon-dependent innate immunity. *Nature* **461**, 788–792 (2009).
16. Li, X.D. *et al.* Pivotal roles of cGAS-cGAMP signaling in antiviral defense and immune adjuvant effects. *Science* **341**, 1390–1394 (2013).
17. Paludan, S.R., Bowie, A.G., Horan, K.A. & Fitzgerald, K.A. Recognition of herpesviruses by the innate immune system. *Nat. Rev. Immunol.* **11**, 143–154 (2011).
18. Crotta, S. *et al.* Type I and type III interferons drive redundant amplification loops to induce a transcriptional signature in influenza-infected airway epithelia. *PLoS Pathog.* **9**, e1003773 (2013).
19. Leib, D.A. *et al.* Interferons regulate the phenotype of wild-type and mutant herpes simplex viruses *in vivo*. *J. Exp. Med.* **189**, 663–672 (1999).
20. Mordstein, M. *et al.* Interferon-λ renders epithelial cells of respiratory and gastrointestinal tract resistant to viral infections. *J. Virol.* **84**, 5670–5677 (2010).
21. Zhao, X. *et al.* Vaginal submucosal dendritic cells, but not Langerhans cells, induce protective T_H1 responses to herpes simplex virus-2. *J. Exp. Med.* **197**, 153–162 (2003).
22. Groom, J.R. & Luster, A.D. CXCR3 ligands: redundant, collaborative and antagonistic functions. *Immunol. Cell Biol.* **89**, 207–215 (2011).
23. Cheshenko, N. *et al.* HSV activates Akt to trigger calcium release and promote viral entry: novel candidate target for treatment and suppression. *FASEB J.* **27**, 2584–2599 (2013).
24. Radhakrishnan, P. *et al.* Immature truncated O-glycophenotype of cancer directly induces oncogenic features. *Proc. Natl. Acad. Sci. USA* **111**, E4066–E4075 (2014).
25. Bagdonaite, I. *et al.* A strategy for O-glycoproteomics of enveloped viruses–the O-glycoproteome of herpes simplex virus type 1. *PLoS Pathog.* **11**, e1004784 (2015).
26. McGuckin, M.A., Linden, S.K., Sutton, P. & Florin, T.H. Mucin dynamics and enteric pathogens. *Nat. Rev. Microbiol.* **9**, 265–278 (2011).
27. Harrington, S.M. *et al.* The Pic protease of enteroaggregative *Escherichia coli* promotes intestinal colonization and growth in the presence of mucin. *Infect. Immun.* **77**, 2465–2473 (2009).
28. Frazer, L.C., O'Connell, C.M., Andrews, C.W. Jr., Zurenski, M.A. & Darville, T. Enhanced neutrophil longevity and recruitment contribute to the severity of oviduct pathology during Chlamydia muridarum infection. *Infect. Immun.* **79**, 4029–4041 (2011).
29. Archer, N.K., Harro, J.M. & Shirtliff, M.E. Clearance of *Staphylococcus aureus* nasal carriage is T cell dependent and mediated through interleukin-17A expression and neutrophil influx. *Infect. Immun.* **81**, 2070–2075 (2013).
30. Milligan, G.N. Neutrophils aid in protection of the vaginal mucosae of immune mice against challenge with herpes simplex virus type 2. *J. Virol.* **73**, 6380–6386 (1999).
31. Jenne, C.N. *et al.* Neutrophils recruited to sites of infection protect from virus challenge by releasing neutrophil extracellular traps. *Cell Host Microbe* **13**, 169–180 (2013).
32. Ohmori, Y., Schreiber, R.D. & Hamilton, T.A. Synergy between interferon-γ and tumor necrosis factor-α in transcriptional activation is mediated by cooperation between signal transducer and activator of transcription 1 and nuclear factor-κB. *J. Biol. Chem.* **272**, 14899–14907 (1997).
33. Ohmori, Y. & Hamilton, T.A. The interferon-stimulated response element and a κB site mediate synergistic induction of murine IP-10 gene transcription by IFN-γ and TNF-α. *J. Immunol.* **154**, 5235–5244 (1995).
34. Hollingsworth, M.A. & Swanson, B.J. Mucins in cancer: protection and control of the cell surface. *Nat. Rev. Cancer* **4**, 45–60 (2004).
35. Dodds, P.N. & Rathjen, J.P. Plant immunity: towards an integrated view of plant-pathogen interactions. *Nat. Rev. Genet.* **11**, 539–548 (2010).

ONLINE METHODS

Animals. Specific pathogen-free C57BL/6 (WT), *Tlr3*$^{-/-}$, *Tlr2*$^{-/-}$*Tlr9*$^{-/-}$, STING-Goldenticket (*Tmem173*$^{gt/gt}$) and *Il28ra*$^{-/-}$ mice were bred at Taconic M&B, Ry, DK. *Ifnar1*$^{-/-}$, *Ifngr*$^{-/-}$ and *Cxcr3*$^{-/-}$ mice were bred at the Panum Institute, University of Copenhagen. *Irf3*$^{-/-}$; *Irf7*$^{-/-}$ and *Mavs*$^{-/-}$ mice were bred at Université Libre de Bruxelles, and *Card9*$^{-/-}$ mice were bred at the Technische Universität München. All experiments were carried out at University of Aarhus. Prior to experiments, mice were kept at the animal facility Faculty of Health Science, University of Aarhus for 7–8 d. All mice used in this study were age-matched (7–12 weeks of age) female mice on a C57BL/6 background. Isoflurane (Abbott) was used to anesthetize mice, and all mice were pre-treated with Depo Provera (Pfizer). Ethical permission was obtained from the Danish Veterinary and Food Administration to perform the vaginal and ocular HSV infections. All efforts were made to minimize suffering, and mice were monitored daily during infection.

Viruses, bacteria and reagents. The viruses used were HSV-2 (laboratory strains 333 and G and clinical isolate 90.036, Sweden), gD-deficient HSV-2 (strain G) (HSV-2 ΔgD, grown in Vero cells; HSV-2 ΔgD-R, grown in gD-expressing Vero cells)[23], and HSV-1 (strain McKrae). Vero cells used were from the lab stock; wild-type and *COSMC* knockout HaCaT cells were obtained from H. Wandall (Copenhagen University). All cell lines were tested negative for mycoplasma within 6 month before submission of the manuscript. The viruses were propagated using standard conditions[13]. Mouse-derived HSV-2 was produced by harvest of supernatants from murine neurons infected for 48 h with HSV-2. For UV inactivation, HSV-2 was placed in a 24-well plate on ice and exposed to UV light for 35 s. For heat inactivation, the virus was incubated for 30 min at 65 °C. The efficiency of inactivation was controlled by viral plaque titration on Vero cells. *E. coli* (EAEC, strain 042 and the ΔPic mutant) were propagated as described[27]. Growth medium used was Eagle's Minimal Essential Medium (MEM), Iscoves Modified Dulbecco's Medium (IMDM) (both from BioWhittaker) and CnT-basal medium (CELLnTEC). MEM was supplemented with 2% glutamine, 0.5% nystatin, 200 IU/mL penicillin, 200 μg/mL streptomycin, 0.1% gentamycin, 10% $NaHCO_3$ and 2–5% heat-inactivated FCS (BioWittaker). CnT-basal medium was supplemented with 200 IU/mL penicillin, 200 μg/mL streptomycin and CnT19 supplements (CELLnTEC).

Production of virus lacking elongated O-linked glycans. To produce HSV-2 (strain 333) lacking elongated O-linked glycans we used *COSMC* konckout (KO) HaCaT cells[24]. Briefly, parental HaCaT and *COSMC*-deficient HaCaT cells were seeded at density of 80–90% confluence. The cells were infected with HSV-2 at multiplicity of infection (MOI) 0.01, and the infection was left to progress to ~95% cytopathic effect, at which point the cells were frozen (−70 °C). After thawing, supernatants were centrifuged at 5,000 r.p.m. for 60 min and ultracentrifugated at 12,500 r.p.m for 4 h at 4 °C to pellet the virus. The viruses were resuspended in DMEM supplemented with 5% FCS. The virus derived from the two cell lines was titrated on monolayer of Vero cells. To assess the effect of O-linked O-glycans on virion stability, we produced viruses in the presence of 3 μM deoxy-5-ethynylcytidine in the growth medium. The viruses grown in HaCaT and *COSMC* KO cells were incubated at 37 °C for 30 min in medium. The viruses were fixed onto poly-L-lysine–coated coverslips, and viral DNA and capsids were detected using the Click-iT Imaging Kit (Invitrogen) and anti-VP5. Images were acquired on a Zeiss LSM 710 confocal microscope using a 63× 1.4 oil-immersion objective, and image processing was performed using Zen 2010 (Zeiss).

Enzymatic removal of glycans from HSV-2. HSV-2 (strain 333) grown in Vero cells was deglycosylated by use of enzyme deglycosylations kits (New England BioLabs) according to the instructions of the manufacturer. Removal of both N-linked and O-linked glycans was conducted by use of a protein deglycosylation mix of PNGase F, O-glycosidase, neuraminidase, β1-4 galactosidase and β-*N*-acetylglucosaminidase. N-linked oligosaccharides were removed by use of PNGase F (15,000 units) and O-linked oligosaccharides by use of a series of exoglycosidases (O-glycosidase (2,000,000 units), neuraminidase (2,000 units), β1-4 galactosidase (400 units) and β-*N*-acetylglucosaminidase (100 units)). Briefly, native deglycosylation of virus was achieved by incubation of 180 μL HSV-2 virus with the respective enzymes for 4 h at 37 °C and subsequently centrifuged for 3 h at 12,500 r.p.m. and resuspended in 180 μL DMEM 5% FCS. For 180 μL HSV-2 virus, 20 μL of 10× G7 reaction buffer (New England Biolabs) and 20 μL of deglycosylation enzyme cocktail mix were used. For removal of O-linked oligosaccharides the 10× G7 buffer was used. As a control an aliquot of virus was subjected to the denaturing protocol to provide a positive protocol for the fully deglycosylated protein. The virus was subsequently ultracentrifuged and resuspended to remove enzymes and free glycans before use in experiments. The extent of deglycosylation was assessed by mobility shift on SDS-PAGE gels using antibodies against gB and gD (Virusys). Mice were infected with the enzyme-treated viruses as described below.

Mass spectrometry. To determine the the O-glycoproteome of HSV-2, pellet from two confluent 175-cm^2 flasks infected with HSV-2 (333) to >90% cytopathic effects were used. First, lectin weak-affinity chromatography (LWAC) was performed as described[25] to capture T- and Tn-glycopeptides. LWAC fractions were screened by preliminary liquid chromatography–mass spectrometry (LC-MS), and those most enriched in glycopeptides were pooled and further fractionated by isoelectric focusing. Half of the PNA-enriched material was subjected to chymotrypsin (Roche) digestion (0.1 μg overnight at 37 °C) to further break down high–molecular weight peptides. Mass spectrometry analysis was performed on an EASY-nLC 1000 UHPLC (Thermo Scientific) interfaced via nanoSpray Flex ion source to an Orbitrap Fusion MS (Thermo) as described[25]. MS1 precursors were detected at a nominal resolution of 120,000. MS2 spectra (m/z of 75–2,000) were acquired at a resolution of 60,000 for both HCD and ETD. Isolation width was set to m/z of 3 (quadrupole). Automatic gain control targets were 5×10^4 for MS1 and 1×10^5 for MS2 scans. Supplemental activation of charge-reduced species in the ETD was 25%. In all cases the precursor mass tolerance was set to 5 p.p.m., and fragment ion mass tolerance to 20 mmu.

Vaginal HSV-2 infection. The mice were pretreated by subcutaneous (s.c.) injection of 2 mg of Depo-Provera (Pfizer). Five days later mice were anesthetized with Isoflurane (Abbott) and inoculated intravaginally with 20 μL HSV-2 (6.7×10^4 p.f.u.) suspended in IMDM. Mice were then placed on their backs and maintained under anesthesia for 10 min. Vaginal washes were collected after infection (p.i.) by washing with 2 × 40 μL of IMDM and dilution to a final volume of 250 μL. In separate experiments, mice were euthanized by cervical dislocation (c.d.) at different time points after infection, and vaginas were isolated and used for RNA extraction, flow analysis or immunohistochemistry. Infected mice were observed and examined daily and scored for vaginal inflammation, neurological illness, and death. The severity of disease was scored according to the following scale: 0, healthy; 1, genital erythema; 2, moderate genital inflammation; 3, purulent genital lesion/or generally bad conditions; 4, hindlimb paralysis or generally very poor condition. Mice were sacrificed by c.d. at score 4.

Ocular HSV-1 infection. Mice were anesthetized intraperitoneally with ketamine and xyalazine. Corneas were bilaterally scarified and inoculated with virus by adding 2×10^6 p.f.u. of HSV-1 (strain McKrae) per eye in a 5-μl volume. Eyes were isolated 24 h p.i. and placed in RPMI medium for 1 h, at which point protein levels of CXCL10 and IFN-α/β in the medium were measured.

Isolation and culture of vaginal epithelial monolayer. Vaginas were excised from female mice and treated with collagenase/dispase (Roche) (1 mg/ml) for 2–3 h. Subepithelial tissue was removed at a width of no more than 1 mm, and the cell layer was cultured in CnT medium. More than 95% of the cells in the cell layer were negative for CD45 as assessed by flow cytometry (data not shown).

Physical and enzymatic disturbance of the vaginal mucosa. The mice were pretreated by s.c. injection of 2 mg Depo-Provera (Pfizer). Five days later, mice were anesthetized with isoflurane (Abbott). For physical disturbance of the vaginal mucosa, mice were flushed intravaginally three times with 25 μL PBS. To disturb the mucosa enzymatically, mice were administered 1.6 units (0.2 μg) of hyaluronidase from *Streptococcus pyogenes* (Sigma-Aldrich) in

20 µL intravaginally. Vaginal washes were collected and analyzed as described above.

Depletion of neutrophils *in vivo*. To deplete neutrophils *in vivo*, mice were treated intraperitoneally with 500 µg anti-Ly6G (clone 1A8) or isotype control (BioXCell). Twenty-four hours later, mice were infected as described above. The efficiency of neutrophil depletion in the vaginal tissue was evaluated by flow cytometry.

Virus plaque assay. Vaginal washes were collected from mice infected intravaginally with HSV-2 or uninfected (UN) mice and immediately placed on dry ice and then stored at −70 °C until used for analysis. Viral titers of vaginal washes were determined on monolayers of Vero cells seeded in MEM supplemented with 5% FCS at a density of 1.2×10^6 cells per well and left overnight to settle. The next day the cells were infected with 100 µL serially diluted vaginal washes. The cells were incubated for 1 h, then 5 mL MEM supplemented with 0.2% human immunoglobulin (ZLB Behring GmBH) was added. The plates were further incubated for 2–3 d and stained with 0.03% methylene blue in order to count the plaques. The results were expressed as p.f.u. per vaginal wash.

IFN-α/β bioassay. IFN-α/β bioactivity was measured by use of a L929 cell–based bioassay. Vaginal washes and murine IFN-α/β standard was added to 96-well plates in successive two-fold dilutions. Prior to use, HSV-2 in vaginal samples was inactivated by UV light treatment for 6 min. L929 cells (2×10^4 cells/well) were added to each well, and the plates were incubated overnight at 37 °C. The next day vesicular stomatitis virus (VSV/V10) was added to the wells, and the plates were further incubated for 2–3 d. The dilution mediating 50% protection was defined as 1 U of IFN-α/β per ml. The bioassay had a detection limit of 6 U/ml.

Cytokine measurements. Vaginal washes were used for measurement of cytokines by ELISA and Luminex, according to the instructions of the manufacturer. Mouse CXCL10, CXCL9, CCL5, IL-6, IFN-λ and IFN-γ were all detected by use of DuoSet ELISA Development System from R&D. Mouse CCL2, CXCL1, IL-1β, IL-10 TNF-α, IL-15 and IL-33 were measured by Luminex Technology using kits from Bio-Rad.

***In vitro* HSV-2 infection.** Vaginas were isolated from mice and cut lengthwise and subsequently suspended in 4 mL collagenase/dispase (1 mg/mL) and incubated on an orbital shaking table for 3 h at 37 °C. The enzyme activity was stopped by PBS supplemented with 0.02% EDTA. The epithelial layer was separated from the underlying basement membrane and incubated in CnT-19 medium before stimulation with 2.1×10^7 p.f.u./mL HSV-2. After infection with HSV-2, the epithelial cell layer was homogenized in lysis buffer (Roche) and RNA was extracted by use of High Pure RNA Isolation Kit (Roche).

Quantitative RT-PCR. mRNA encoding CXCL10, IFN-β, IFN-α4, cGAS, Muc1, Muc2, Muc5b, A20, GAPDH, gB, and β-actin was quantified by using TaqMan Gene Expression Assay (Applied Biosystems) according to manufacturer's recommendations. Total RNA from isolated vaginas was extracted with TRIzol (Invitrogen) according to the recommendations of the manufacturer. Vaginal tissue was homogenized in TRIzol and chloroform was added, followed by phase separation by centrifugation. RNA was precipitated with isopropanol and pelleted by centrifugation. Pellets were washed with 80% ethanol and dissolved in RNase-free water. For cDNA generation, RNA was subjected to reverse transcription (RT) with oligo(dT) as primer and Expand Reverse Transcriptase (both from Roche). Prior to qRT-PCR, RNA was treated with DNase I (Ambion) to remove any contaminating DNA, the absence of which was confirmed in control experiments in which the reverse transcriptase enzyme was omitted. The expression of PRRs mRNA was quantified using SYBR Green (Stratagene) with the following primers: Mouse TLR2, forward: 5′-GGCTCTTCTGGATCTTGGTG-3′, reverse: 5′-GAGTCCGGAGGGAATAGAGG-3′. Mouse TLR3, forward: 5′-CTCT TGAACAACGCCCAACT-3′, reverse: 5′-GTCCACTTCAGCCCAGAGAA-3′. Mouse TLR9, forward: 5′-CATGGACGGGAACTGCTACT-3′, reverse: 5′-GGCACCTTTGTGAGGTTGTT-3′. Mouse RIG-I, forward: 5′-ATGGC AGACAAAGAGGAGGA-3′, reverse: 5′-TCGTGGAAGAAGGCTTTGAG-3′. Mouse Mda-5, forward: 5′ ACAGAGGCCTGG AACGTAGA-3′, reverse: 5′-CTGCCCATGTTGCTGTTATG-3′. Mouse β-actin, forward: 5′-TAGCA CCATGAAGATCAAGAT-3′, reverse: 5′-CCGATCCACACAGAGTACTT-3′. Mouse dectin1, forward:5-GGAATCCTGTGCTTTGTGG-3′, reverse: 5′-TAG TTTGGGATGCCTTGGAG-3′. Mouse dectin2, forward: 5′-CTGCCCA AATCACTGGAAGT-3′, reverse: 5′-ATCCGAAAGACCCAGGAAGT-3′. CD209a, forward: 5′-GGCTTCCAAACAAATTCTGG-3′, reverse: 5′-TTCAACT GGGTCAGTTCTTGG-3′. CD209c, forward: 5′-CCTCTGCAATCAAGCT CTCC-3′, reverse: 5′-ATGCGCATGTATGTTTGTGG-3′. CD209d, forward: 5′-CTGTCACCCAGCTTTACACGC-3′, reverse: 5′-AGATCATTCCAG CCATCCCCA-3′. CD209e, forward: 5′-AGATGGGCTCTCTGGGATTTC-3′, reverse: 5′-AGCTGGGCATCTTGGAAACT-3′. CD209f, forward: 5′-CTGGAG AGCAGGGATTTGC-3′, reverse: 5′-GCTGATCCTGGGTCTGTCC-3′. CD209g, forward: 5′- ACACCCCACTCAAACTCAGC-3′, reverse: 5′-AAGTT GCCTGTGTGGCTAGG-3′. Mannose receptor, forward: 5′-CATCAGAG CCTGGAAAGAGC-3′, reverse: 5′-TAGGGCCACCACTGATTAGG-3′. Mingle, forward: '5-TCGGACCAATCTCACTTTCC-3′, reverse: 5′-CCAGGAAAG GATGACACAGC-3′. MDL1, forward: 5′-TTCTCCTTCTCCGAATCACC-3′, reverse: 5′-TCTCTCCAGGCTGACGTACC-3′.

Immunohistochemistry of murine vagina. Vaginas were removed and placed in 2–4% formaldehyde in PBS and fixed for 24 h. The tissue was embedded in paraffin and 2-µm sections were cut from tissue blocks on a microtome (Leica). Sections were rehydrated in ethanol, and endogenous peroxidase enzymes were blocked using absolute methanol with 0.5% hydrogen peroxide (H_2O_2). Sections were boiled in microwave in 10 mM Tris, 0.5 mM EGTA (pH 9.0) to reveal antigens, and the free aldehyde groups were blocked by 50 mM NH_4Cl in PBS. Sections were washed in buffer A (0.01 M PBS, 1% BSA, 0.2% gelatine, and 0.05% saponin) and incubated with primary antibody in buffer B (0.1% BSA, 0.3% Triton X-100 in PBS) overnight at 4 °C. After another round of wash with buffer A, the sections were incubated with HRP-conjugated secondary antibody (P448, DAKO) in buffer B. Antibody binding was visualized by use of 3,3′-diaminobenzidine (Kem-En-Tec) in 0.03% H_2O_2 and sections were counterstained with Mayer's or Harris's hematoxylin solution (Sigma Aldrich), followed by dehydration and mounted using Eukitt reagent (Eukitt, O. Kindler GmbH and Company). The primary antibodies used for light microscopy were polyclonal rabbit anti-HSV-2 (Dako) (1:100–250) and rabbit anti-CXCL10 (BS-1502R, NordicBiosite, 1:900). For periodic acid–Schiff stainings, vaginal epithelium was fixed by immersion in Carnoy's fixative, (60% ethanol, 30% chloroform, 10% acetic acid), dehydrated in a graded ethanol series (70%, 96%, 99% ethanol, 2 h per concentration) and xylene (2 h) before embedded in paraffin. Sections were cut at 2 µm, dewaxed in xylenes and redydrated through 99%, 96% and 70% ethanol. Periodic acid–Schiff staining was performed by applying 1% periodic acid for 10 min and Schiff's reagent (Merck 1.09033.0500) for 10 min. Counterstaining was performed hematoxylin for 3 min before the sections were dehydrated and mounted with coverslips. Light microscopy was carried out using a Leica light microscope.

Flow cytometry. Single-cell suspensions of mouse vagina were obtained by enzymatic and mechanic processing in 4 mL collagenase/dispase (1 mg/mL) and 2 mL DNase 1 (2 mg/mL) and incubation under constant stirring at 37 °C for 45 min. The tissue suspension was then gently mashed and filtered through a 70-µm (pore size) mesh (BD Falcon) and then passed through a 40-µm (pore size) mesh and washed with PBS with 0.02% EDTA to stop enzyme activity. Cells were centrifuged for 8 min at 1,600 r.p.m. and resuspended in 200 µL PBS per vagina. Before staining the cells were blocked for 10 min with anti-mouse CD16/CD32 antibody (eBioscience) and mouse or rat IgG (Jackson ImmunoResearch). Cells were incubated with primary antibodies for 30 min on ice in the dark and washed in PBS. The cells were resuspended in 250 µL 1% formaldehyde in PBS. The following primary anti-mouse antibodies were used for flow identification of cell populations; CD45-APC (Clone 30-F11), NK1.1-FITC (clone PK136), Nk1.1-PE (Clone PK136), CD11b-PE (clone M1/70), Ly-6g-APC (clone 1A8), APC RAT IgG2b, κ-isotype, FITC RAT IgG2a, κ-isotype and PE RAT IgG2a, κ-isotype and 7-AAD (live/dead cell marker), all from BD Pharmingen. Flow-count beads (Beckman Coulter)

doi:10.1038/ni.3319

were added to the flow samples just before analysis. The cells were analyzed on FC500 flow cytometer (Beckman Coulter) or FACsAria III (BD Biosciences) and data was processed with FlowJo version 7.6.5 (TreeStar). In all cases where data are presented for infected mice only, no differences were observed between the genotypes compared for the read-out presented.

Immunoblotting. Vaginal tissues or epithelial cell layers were lysed in RIPA buffer in the presence of protease and phosphatase inhibitors then subjected to homogenization and centrifugation. The cleared supernatants were sonicated, and samples were subjected to SDS-PAGE and immunoblotting. The blots were blocked with 2.5% BSA and probed with the following primary antibodies: CXCL10 (R&D, AF-466-NA), pSTAT1 (Cell Signaling, 7649), viperin (Millipore, MABF106) and vinculin (Sigma, V9131). Dilutions and catalog numbers were as follows: goat anti-CXCL10, 1:500, AF-466-NA; rabbit anti-pSTAT1, 1:1,000, 7649; mouse anti-viperin, 1:800, MABF106; mouse anti-vinculin, 1:1,000, V9131. Appropriate peroxidase-conjugated secondary antibodies were used for development (Jackson ImmunoResearch). Secondary antibodies were as follows: anti-goat, catalog no. 705-306-147; anti-rabbit, catalog no. 711-035-152; anti-mouse, catalog no. 715-036-150 (all used at dilution 1:10,000).

Statistics. For statistical analysis of data on cytokines, chemokines and virus titers we used two-tailed Students *t*-test when the data exhibited normal distribution and Wilcoxon rank-sum test when the data set did not pass the normal distribution test. Comparison of groups with regard to mean disease score was done on the basis of simulated 95% confidence intervals from the nonlinear mixed effects regression model[36]. *P* values were calculated from the confidence intervals assuming normally distributed mean group differences. *P* values ≤ 0.05 were considered to reflect statistically significant differences between compared groups. Symbols for *P* values used in the figures: $^{*}P < 0.05$, $^{**}P < 0.01$, $^{***}P < 0.001$. The data shown are representative from one out of three or more experiments. No animals were excluded from the analysis. No method was used to randomize animals between groups. Scoring of disease development in animals was performed blinded.

36. Pinheiro, J.C. & Bates, D.M. in *Mixed Effects Models in S and S-PLUS* 273–301 (Springer, 2000).